

Preparation of Flowerlike Porous $\text{Mg}_5(\text{CO}_3)_4(\text{OH})_2 \cdot 4\text{H}_2\text{O}$ by CO_2 Bubble Templating

LEI Hong¹, WEI Yu¹, HUANG Zhiliang*¹, KONG Shijin¹ and YAO Donghui¹

¹School of Materials Science and Engineering, Wuhan Institute of Technology, Wuhan 430074, People's Republic of China

* correspondence: hzl6455@126.com

Abstract: Flowerlike porous basic magnesium carbonate ($\text{Mg}_5(\text{CO}_3)_4(\text{OH})_2 \cdot 4\text{H}_2\text{O}$) were obtained successfully using magnesium chloride hexahydrate and ammonium bicarbonate as raw materials. We investigated the effect of reaction time and reaction temperature on the $\text{Mg}_5(\text{CO}_3)_4(\text{OH})_2 \cdot 4\text{H}_2\text{O}$ preparation. In the first three hours' reaction, Magnesium carbonate trihydrate ($\text{MgCO}_3 \cdot 3\text{H}_2\text{O}$) whiskers generated, and transferred to the flowerlike porous $\text{Mg}_5(\text{CO}_3)_4(\text{OH})_2 \cdot 4\text{H}_2\text{O}$ as the reaction time prolonged. During the transformation, the flowerlike $\text{Mg}_5(\text{CO}_3)_4(\text{OH})_2 \cdot 4\text{H}_2\text{O}$ crystals firstly appeared at the head of the $\text{MgCO}_3 \cdot 3\text{H}_2\text{O}$ whisker.

1. Introduction

The morphology and properties of particles are closely related. To fabricate materials with certain morphology to achieve better performance, there has been increasing interests in controlled synthesis of inorganic microstructure with desirable shape and size[1-2].

Because of the special structure, spherical porous materials have advantages in easily moving, closely packing and occupying the available vacancies, which implies potential applications[3]. In recent years, in particular, spherical porous materials have attracted much attention and many studies have been carried out on the superiority of spherical porous materials. For example, Wang et al. have synthesized spherical porous CaCO_3 microparticle which could be applied as relatively safe drug vehicles. Yu *et al* have prepared spherical porous LiFePO_4/C particles which provide better contact with electrolyte and are easier to bind than isolated LiFePO_4 particles[4-5].

This paper presents the formation process of flowerlike porous $\text{Mg}_5(\text{CO}_3)_4(\text{OH})_2 \cdot 4\text{H}_2\text{O}$. By investigating particles under various reaction times, the shape evolution of these flowerlike porous particles is discussed in detail. CO_2 bubble template was introduced to simulate the formation of flowerlike porous $\text{Mg}_5(\text{CO}_3)_4(\text{OH})_2 \cdot 4\text{H}_2\text{O}$, and the equation of reaction temperature and the pore size was given by the derivation of Laplace and Clapyeron equations.

2. Experimental

Magnesium chloride hexahydrate ($\text{MgCl}_2 \cdot 6\text{H}_2\text{O}$) and ammonium bicarbonate (NH_4HCO_3) were used and were of analytical grade. In this experiment, 0.4 mol/L of $\text{MgCl}_2 \cdot 6\text{H}_2\text{O}$ and NH_4HCO_3 (1/2 molar ratio of $\text{MgCl}_2 \cdot 6\text{H}_2\text{O}$) were mixed well and transferred into automatic Control Reaction Kettle. Then, the homogeneous reaction solution was heated at a constant pressure of 4 atm. The reaction temperature was maintained at 80 °C for a given reaction time. The reaction time was set as 3~6 h. After reaction finished, the special autoclave was taken out for ageing for 3 h. Afterwards, a filtration



was implemented by vacuum suction filter method and washed with distilled water as well as ethanol. The washed residue was dried in vacuum oven for 2 h.

The crystal phases of the products were determined by XD-5A-type powder X-ray diffraction (XRD) with Ni-filtered Cu K α radiation. The morphology of the product was observed using a JSM-5510LV scanning electron microscope (SEM).

3. Results and discussion

Figure. 1 shows XRD patterns of the mixtures produced under 80 °C for different duration times. The XRD pattern of the mixture prepared by reacting 3 h displays only the peaks of MgCO₃·3H₂O. The XRD pattern of the mixture obtained after reacting 4 h are dominated by the peaks of MgCO₃·3H₂O, with the main characteristic peaks of Mg₅(CO₃)₄(OH)₂·4H₂O just starting to show up in the XRD. 5 h later, Mg₅(CO₃)₄(OH)₂·4H₂O becomes the dominant phase in the mixture. Mg₅(CO₃)₄(OH)₂·4H₂O is the only phase present in the XRD pattern of the mixture when reaction time was increased to 6 h.

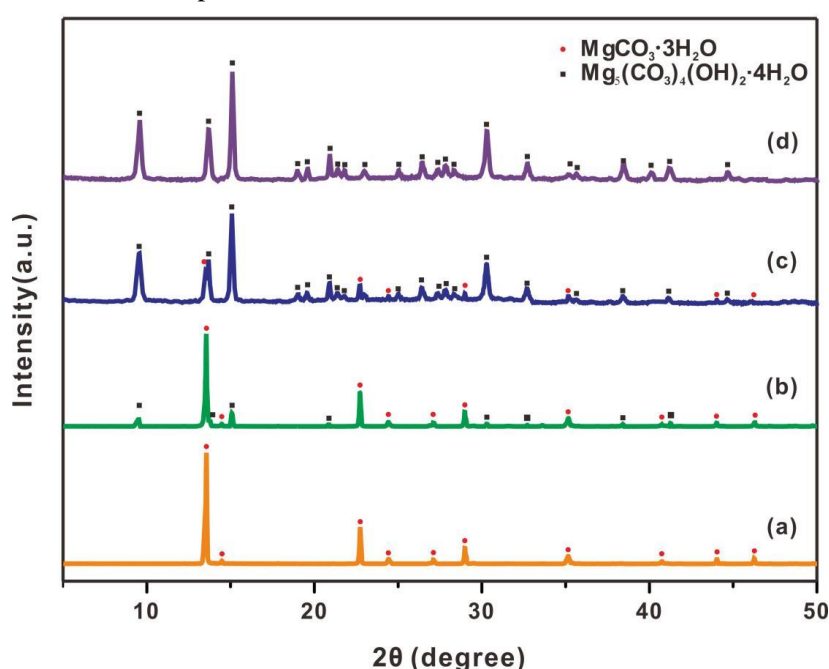


Figure 1. XRD patterns of the heated mixtures at 80 °C for different duration times (a: 3 h; b: 4 h; c: 5 h; d: 6h)

Figure. 2 shows SEM images of the particles synthesized at different reaction time, which indicates an obvious growth process occurring from whisker to flowerlike microsphere with porous structure. As shown in Fig. 2a, a large number of whiskers were obtained by reacting 3 h. Through the phase analysis, the product was determined as MgCO₃·3H₂O (Fig. 1a). The structure and surface of MgCO₃·3H₂O whiskers were unbroken and smooth. In addition, the length was about 140 μm and the aspect ratio was about 25. At the time of reacting 4 h, the sample was still whisker with reduced aspect ratio, but the surface became rough and a small number of leaf-like crystals appeared on the surface of the whisker. When the reaction time was increased to 5 h, the sample not only contained whisker product, but also began to appear flowerlike spherical particles. From a magnifying SEM image, it seemed that “connected flakes” gathered on the head of the whisker (Fig. 2c). When the samples were produced for reacting 6 h, the original whisker shape disappeared completely. All samples turned into the flowerlike porous Mg₅(CO₃)₄(OH)₂·4H₂O that are assembled by lamella (Fig. 2d).

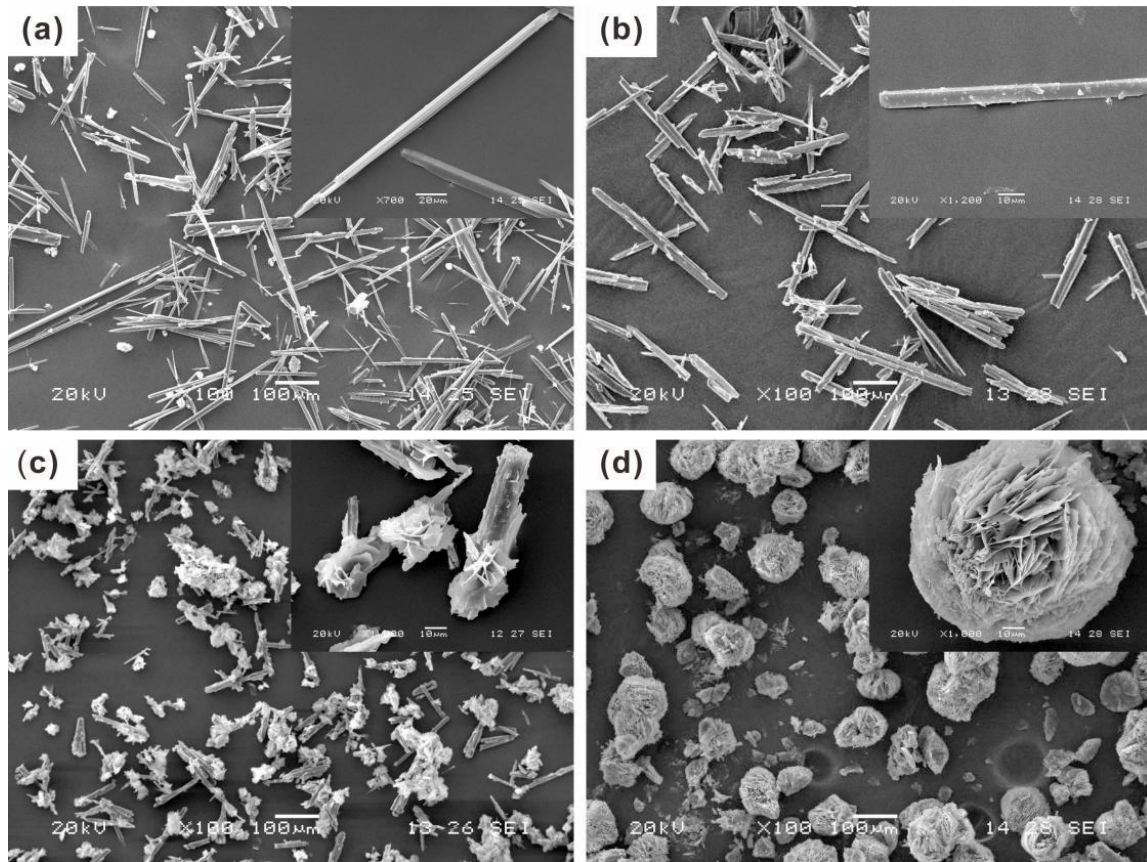
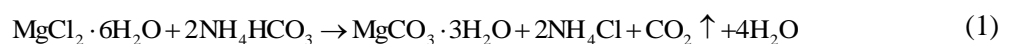


Figure 2. SEM images of the particles synthesized at different reaction time (a: 3 h; b:4 h; c: 5 h; d: 6 h)

The conversion reaction giving rise to the $\text{Mg}_5(\text{CO}_3)_4(\text{OH})_2 \cdot 4\text{H}_2\text{O}$ crystal occurs via the formation of metastable $\text{MgCO}_3 \cdot 3\text{H}_2\text{O}$ in the synthetic process[6-8]. The reaction time has a significant impact on the phase transition process. Reactions of the transition process occur as follows:



As shown in Figure. 2d, the surfaces of the flowerlike $\text{Mg}_5(\text{CO}_3)_4(\text{OH})_2 \cdot 4\text{H}_2\text{O}$ are assembled from a number of lamellae that interconnected to form an open porous structure. Generally, gas bubbles, such as CO_2 bubbles, can form open porous structure [9]. With the increase of reaction time, the NH_4HCO_3 slowly releases CO_2 bubbles. At the same time, in order to obtain lower surface tension to achieve a relatively stable state, small CO_2 bubbles gather into big spheres of micrometer size and preferentially adhere to the head of whisker (see Figure. 3). This process can be explained by Gibbs function:

$$dG = -SdT + Vdp + \sum_{\alpha} \sum_B \mu_{B(\alpha)} dn_{B(\alpha)} + \gamma dA_s \quad (3)$$

where G , S and V are Gibbs function, entropy and volume of system, separately; μ_B and n_B are chemical potential and amount of substance of component B in phase A , respectively; A_s is the interfacial area; γ is the interfacial tension. Since the temperature and pressure are constant, equation 3 can be simplified as follows:

$$dG = \gamma dA_s \quad (4)$$

If γ remains constant, upon integration equation 4 gives

$$G^s = \gamma A_s \quad (5)$$

Further differential equation can be obtained:

$$dG^s = \gamma dA_s + A_s d\gamma \quad (6)$$

Under the condition of constant temperature and constant pressure, the decrease of Gibbs function of interface system is a spontaneous process from the thermodynamic view. According to the equation 6, In order to reduce the interfacial Gibbs function to achieve relatively stable state, Many small CO₂ bubbles reduce its surface area by gathering into big CO₂ bubbles, and the head of whisker reduce the surface tension by dissolving and adsorbing CO₂ bubbles.

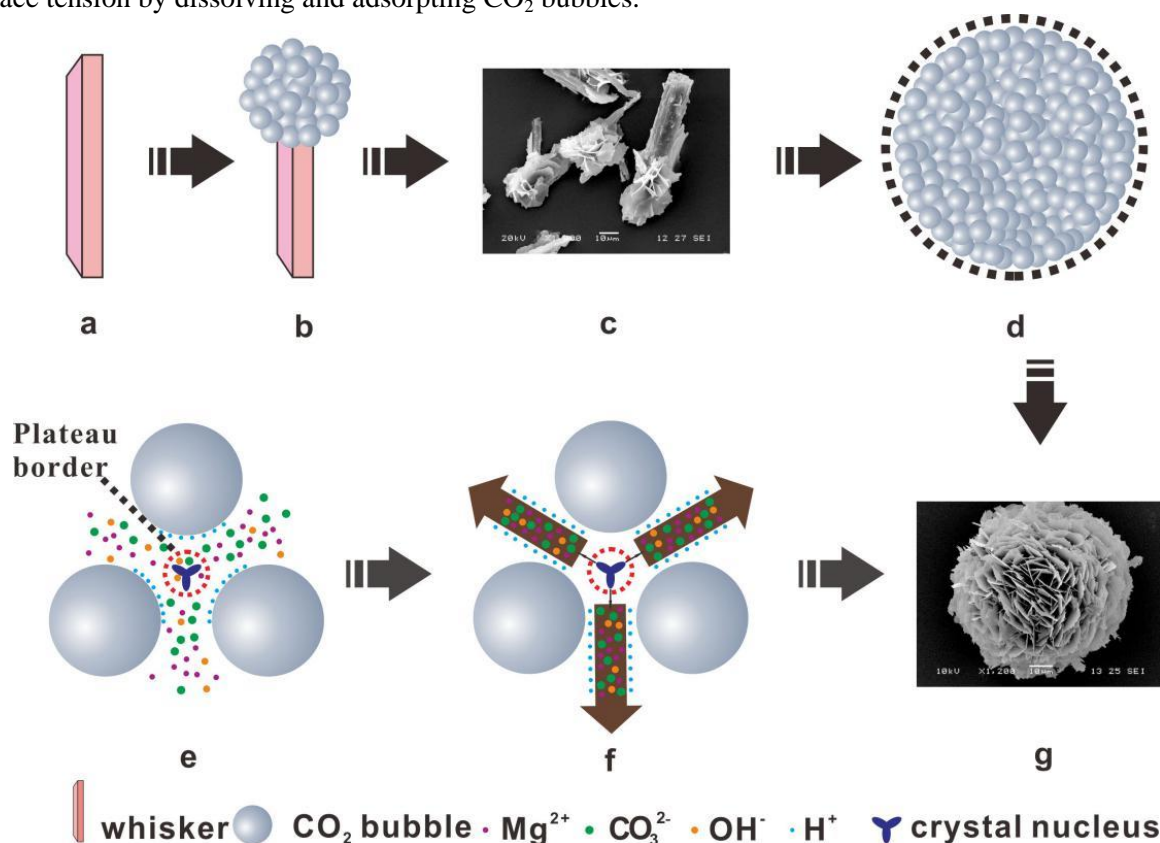


Figure 3. Illustration of the growth process of $Mg_5(CO_3)_4(OH)_2 \cdot 4H_2O$

4. Conclusions

Flowerlike porous $Mg_5(CO_3)_4(OH)_2 \cdot 4H_2O$ have been synthesized successfully using $MgCl_2 \cdot 6H_2O$ and NH_4HCO_3 as raw materials. The formation of porous structure and the control of system temperatures over the pore size of porous $Mg_5(CO_3)_4(OH)_2 \cdot 4H_2O$ were studied.

(1) The products synthesized at 3 h were $MgCO_3 \cdot 3H_2O$ whiskers. After a series of phase transition process, it turned out that the final products for 6 h are flowerlike $Mg_5(CO_3)_4(OH)_2 \cdot 4H_2O$ with porous structure. Moreover, flowerlike $Mg_5(CO_3)_4(OH)_2 \cdot 4H_2O$ crystals firstly appear at the head of the $MgCO_3 \cdot 3H_2O$ whiskers.

(2) The formation of porous structure of flowerlike $Mg_5(CO_3)_4(OH)_2 \cdot 4H_2O$ could be explained. The growth and gathering of the CO₂ bubbles induced the growth of the $Mg_5(CO_3)_4(OH)_2 \cdot 4H_2O$ flakes and formation of the porous structure.

Acknowledgments

This work was supported by the National Natural Science Foundation of China (51374155), the Hubei

Province Key Technology R&D Program (2014BCB034) and the National Natural Science Foundation of Hubei province of China (2014CFB796).

References

- [1] Li G, Zhou M, Ma W W, et al. 2010. Controlled Size and Density Distribution of Nanoparticles by Thermal Ammonia Etching Method[J]. *Journal of Wuhan University of Technology-Mater. Sci. Ed.* 25(1): 108-111.
- [2] Paul W, Sharma C P. 1999. Development of Porous Spherical Hydroxyapatite Granules: Application towards Protein Delivery [J]. *Journal of Materials Science: Materials in Medicine*,10(7): 383-388.
- [3] Wang G, Liu H, Liu J, et al. 2010. ChemInform Abstract: Mesoporous LiFePO₄/C Nanocomposite Cathode Materials for High Power Lithium Ion Batteries with Superior Performance [J]. *Advanced Materials*, 22(44): 4944-4948.
- [4] Yu F, Zhang J, Yang Y, et al. 2010. Porous Micro-Spherical Aggregates of LiFePO₄/C Nanocomposites: A novel and Simple Template-Free Concept and Synthesis Via Sol-Gel-Spray Drying Method [J]. *Journal of Power Sources*, 195(19): 6873-6878.
- [5] Hong M H, Son J S, Kim K M, et al. 2011. Drug-Loaded Porous Spherical Hydroxyapatite Granules for Bone Regeneration [J]. *Journal of Materials Science: Materials in Medicine*, 22(2): 349-355.
- [6] Hopkinson L, Rutt K, Cressey G. 2008. The Transformation of Nesquehonite to Hydromagnesite in the System CaO-MgO-H₂O-CO₂/CaO-MgO-H₂O-CO₂: An Experimental Spectroscopic Study [J]. *The Journal of Geology*, 116(4): 387-400.
- [7] Rautaray D, Sinha K, Shankar S S, et al. 2004. Aqueous Foams as Templates for the Synthesis of Calcite Crystal Assemblies of Spherical Morphology [J]. *Chemistry of Materials*, 16(7): 1356-1361.
- [8] Kim T K, Yoon J J, Lee D S, et al. 2006. Gas Foamed Open Porous Biodegradable Polymeric Microspheres [J]. *Biomaterials*, 27(2): 152-161.
- [9] Cheng X, Huang Z, Li J, et al. 2013, Self-Assembled Growth and Pore Size Control of the Bubble-Template Porous Carbonated Hydroxyapatite Microsphere [J]. *Crystal Growth & Design*, 10(3): 1180-1188.